

2018-01-01

Assessing the size of a twin-cylinder wave energy converter designed for real sea-states

Xu, D

<http://hdl.handle.net/10026.1/11002>

10.1016/j.oceaneng.2017.10.012

Ocean Engineering

Elsevier

All content in PEARL is protected by copyright law. Author manuscripts are made available in accordance with publisher policies. Please cite only the published version using the details provided on the item record or document. In the absence of an open licence (e.g. Creative Commons), permissions for further reuse of content should be sought from the publisher or author.

Assessing the size of a twin-cylinder wave energy converter designed for real sea-states

Dali Xu^{a,1}, Raphael Stuhlmeier^a, Michael Stiassnie^{a,*}

^a*Faculty of Civil and Environmental Engineering, Technion-Israel Institute of Technology, 32000 Haifa, Israel*

Abstract

We discuss the hydrodynamics of a wave energy converter consisting of two vertically floating, coaxial cylinders connected by dampers and allowed to heave, sway and roll. This design, viable in deep water and able to extract energy independent of the incident wave direction, is examined for monochromatic waves as well as broad-banded seas described by a Pierson Moskowitz spectrum. Several possible device sizes are considered, and their performance is investigated for a design spectrum, as well as for more severe sea states, with a view towards survivability of the converters. In terms of device motions and captured power, a quantitative assessment of converter design as it relates to survival and operation is provided. Most results are given in dimensionless form to allow for a wide range of applications.

Keywords: Wave energy; survivability; floating cylinders; broad spectra; deep water.

1. Introduction

The intention of this study is two-fold, providing on one hand a rather comprehensive account of the hydrodynamics of a system of two coaxial, vertically-floating cylinders envisioned as a model for a wave energy converter (WEC), and subsequently assessing the size and survivability of this system for various sea-states. The optimal size of a floating-body WEC will depend significantly on the length of the waves typically encountered. This dependence highlights a major difficulty of floating-body WEC design: the WEC must be small enough to undergo significant motions, and so generate power, and yet large enough to be robust and survive the challenges of the marine environment.

The system proposed here to model a WEC relies on the relative motion of two bodies, rather than on the motion of a body relative to a fixed frame (which may be either the sea bed or a bottom fixed structure), and is termed a *wave-activated body* or *self-reacting device*. Such devices may be installed in

*Corresponding author

Email addresses: xudali@technion.ac.il (Dali Xu), raphael@technion.ac.il (Raphael Stuhlmeier), miky@technion.ac.il (Michael Stiassnie)

¹Present Address: College of Ocean Science and Engineering, Shanghai Maritime University, 1550 Hai Gang Da Dao, 201306 Shanghai, China

12 deep water, where the large distance between the sea-bed and the surface might otherwise be prohibitive.

13 The mooring system for such devices has the sole role of counteracting drift and current forces, allowing
14 the weight of moorings and anchors to be relatively small (see [1] and references therein).

15 Due to their ubiquity in ocean engineering, a rich literature exists on the interaction of water waves and
16 cylindrical bodies. The radiation problem in heave only was addressed by Ursell in [2], and the scattering
17 problem by Dean and Ursell [3]. Miles and Gilbert [4] later employed a variational approximation to
18 provide the far field potential for scattering by a circular dock, along with the lateral forces on the
19 dock. However, their results were subsequently found to contain several inaccuracies, in particular in
20 their calculations of the radiation forces. This prompted Garrett [5] to take up the problem afresh, and
21 establish the scattering forces for a circular dock. Subsequently, Black et al. [6] revisited the application of
22 variational methods to the radiation and scattering problem by several cylindrical geometries, employing
23 Haskind's theorem to give the wave forces. This latter, variational approach did not yield the added
24 mass and damping coefficients. Hence, some years later Yeung [7] studied the radiation problem of a
25 vertical cylinder floating on the water surface and undergoing the combined motions of heave, sway and
26 roll, and obtained these hydrodynamic coefficients. More recently, Bhatta [8] also gave the added mass
27 and damping coefficient of a vertical cylinder undergoing heave motion, in terms of the two dimensionless
28 ratios characterizing the problem (depth to radius and draft to radius). While prior work had focused on
29 the finite depth case, more recently⁹ treated by means of an analytical approximation due to Leppington
30 the forces on a truncated vertical cylinder in water of infinite depth.

31 In the context of wave energy, the consideration of floating cylinders as models of WECs goes back at
32 least to Berggren & Johansson [10], who approximated a device described by Hagerman by two floating,
33 axisymmetric cylinders oscillating in heave, albeit without any considerations of captured power. More
34 recently, Garnaud and Mei [11] revisited the single buoy with the intention of studying it in densely
35 packed arrays, giving the captured power for buoys hanging from a large frame. Such a floating, single-
36 cylinder absorber was also employed by Child and Venugopal [12] in their discussion of optimization of
37 WEC arrays, by Borgarino et al [13] as a generic model to investigate wave interaction effects, and others.
38 Similarly, Teillant et al [14] employ an axisymmetric, heaving two-body device for their study of WEC
39 economics, without detailed hydrodynamic considerations. A slightly different fixed-reference WEC was
40 considered by Engström et al [15], who added a sphere under the floating cylinder. This two-body

1
2
3
4
5
6
7
8
9
10
11
12
13
14
15
16
17
18
19
20
21
22
23
24
25
26
27
28
29
30
31
32
33
34
35
36
37
38
39
40
41 configuration of floating cylinder and submerged sphere was then assumed connected to the sea bed by a
42 generator, and its performance analyzed. Zheng et al [16], in a generalization of Berggren & Johansson
43 to three modes of motion, considered the hydrodynamics of two unconnected, coaxial floating cylinders,
44 again without considering power capture. The power capture for a self-reacting device consisting of two
45 vertical cylinders moving in heave was recently obtained for attacking monochromatic incident waves by
46 Wu et al [17], albeit with a rather terse discussion of their results.

47 The present work combines features of several previous studies, and considers the novel case of two
48 floating cylinders, each allowed to move in all three modes of motion available to an axisymmetric body,
49 connected by an idealized power take-off (PTO) represented by a linear damper of constant charac-
50 teristics.² Subsequent to a detailed description of the wave-structure interaction problem, based on
51 eigenfunction expansion techniques, two main parameters characterizing the device size and damping
52 coefficient are examined. The performance of WECs of different sizes, in terms of explicit values for the
53 motions and captured power, is then given from solutions of the governing equations for various incident
54 waves.

55 We undertake our parametric study with an eye towards applications, and thus also consider irregular
56 waves in the form of a Pierson-Moskowitz (PM) spectrum (see e.g. recent work on optimizing a floating
57 box-barge under irregular waves by Bódai & Srinil [19]). While scatter diagrams may be available for some
58 sites where an assessment of the wave resource has been carried out, where this is not the case estimates
59 based on wind speed will need to be made. To this end, we present our data nondimensionalized on the
60 basis of wind speed, which uniquely determines the PM spectrum. Values of significant wave height and
61 peak period may be readily derived therefrom, and the data recast in these terms if desired. When an
62 incident spectrum is considered, it is no longer possible to assign a simple value to the displacement in
63 heave, sway, and roll of a floating body. To remedy this, the notion of *significant displacement*, derived
64 from the spectral description of the sea surface, is introduced to give some quantitative information about
65 the three motions of the device. This also allows for a measure of survivability for various WEC sizes
66 and sea-states, by examining under which conditions the device displacements grow large. An illustrative
67 grading system is devised to categorize the various performance metrics of the self-reacting WECs.

68 The paper is organized as follows: in Section 2 we present the physical set-up of the problem. This

69
70
71
72
73
74
75
76
77
78
79
80
81
82
83
84
85
86
87
88
89
90
91
92
93
94
95
96
97
98
99
100
101
102
103
104
105
106
107
108
109
110
111
112
113
114
115
116
117
118
119
120
121
122
123
124
125
126
127
128
129
130
131
132
133
134
135
136
137
138
139
140
141
142
143
144
145
146
147
148
149
150
151
152
153
154
155
156
157
158
159
160
161
162
163
164
165

²While studies on PTO control show a promising potential for enhancing performance, particularly for devices with a narrow-banded natural response, practical and robust applications must still be developed (see Hong et al [18]).

69 consists in presenting the twin cylinder WEC and characterizing its geometry, and subsequently presenting
70 the PM spectra for design and survivability considerations. In Section 3 we present, very briefly, the basic
71 mathematical formulation of the governing equations and sketch the solution procedure. Subsequently,
72 we employ the hydrodynamic coefficients and forces found from solving the equations of Section 3 to
73 characterizing WEC design under monochromatic waves in Section 4, and under irregular waves given
74 by a Pierson-Moskowitz spectrum in Section 5. A discussion of these results with a view to applications
75 is given in Section 6, which is subdivided into discussions of power capture, survivability, and a brief
76 synthesis of the preceding sections. Finally, Section 7 presents some concluding remarks and perspectives.

77 2. Physical preliminaries

78 2.1. Geometry

79 The geometry and basic parameters of the twin-cylinder WEC are depicted in Fig 1. The Oxy plane is
80 the still water surface and the z -axis points upwards. (r, θ) are polar coordinates in the horizontal plane,
81 such that $x = r \cos \theta$ and $y = r \sin \theta$. The upper cylinder floats on the water surface with a draft H_1 . To
82 provide for flotation stability, it is important to note that the mass of this cylinder is not uniformly
83 distributed, but is divided into two parts with drafts l_1 and l_2 and densities ρ_1 and ρ_2 , respectively. The
84 lower cylinder is entirely submerged with a draft H_3 , and like the upper cylinder is assumed divided
85 into two parts with densities ρ_3 and ρ_4 and drafts l_3 and l_4 , respectively. The distance between the two
86 cylinders in equilibrium is H_2 . Both of them have the same radius R , and the water depth h is taken
87 to be very large compared to the attacking wave length, with the intention of approximating deep-water
88 conditions.

89 As shown in Fig. 1, the two cylinders are connected by a continuously distributed dashpot, which
90 connects the upper edge of the lower cylinder with the lower edge of the upper cylinder at $r = R$. The
91 integrated dashpot coefficient is C , which results in a dashpot coefficient per length $\frac{C}{2\pi R}$. The dashpot
92 is considered to represent a PTO, which generates energy from both the relative heave and roll motion
93 of the cylinders.³

94 Since the two cylinders are axisymmetric, only these three modes are studied. The heave and sway
95 motions will give rise to relative motions in z and x directions, respectively. For waves propagating in the

60 ³Due to the small effect of sway motions, it is not necessary to consider power take-off in the sway mode for this device
61 geometry.

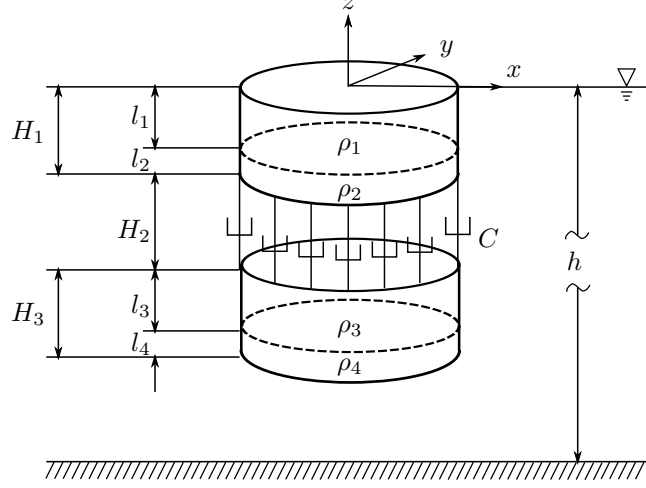


Figure 1: Schematic depiction of the WEC geometry.

x -direction, the two cylinders roll around the y -axis in the mean free surface ($z = 0$), yielding a relative angle about this axis.

This formulation of the problem leaves us with thirteen parameters ($\{H_i \mid i \in \{1, 2, 3\}\}, \{l_j, \rho_j \mid j \in \{1, 2, 3, 4\}\}, R$, and C) characterizing the WEC. Before proceeding, we will make several restrictions to ensure that the problem remains manageable; nevertheless, we shall see that a wealth of interesting phenomena and properties of the WEC are still accounted for.

For simplicity, we will take the drafts and distance between the cylinders identical to their radius, and denote the single size parameter by q , i.e.

$$H_1 = H_2 = H_3 = R \equiv q. \quad (1)$$

For the density distribution of the cylinders, we shall assume

$$\rho_1 = \rho_3 = \frac{3}{4}\rho, \quad \rho_2 = \rho_4 = \frac{3}{2}\rho, \quad l_1 = l_3 = 2l_2 = 2l_4 = \frac{2}{3}q, \quad (2)$$

where ρ is the density of the water. Thus, the design problem is reduced to two parameters, a size q and dashpot coefficient C , whose interplay with incoming waves of certain frequencies is the issue at hand. We shall see that suspending the lower cylinder at a depth $2q$ below the still water surface has the desired effect of rendering its motion rather small, and thus creating a relatively stable point for the upper cylinder to react against.

There are several reasonable criteria which may govern the design of a WEC. Evidently, the WEC should capture as much of the incoming wave energy as possible. At the same time, as economic viability

109 is the prime driver behind wave energy technology, the costs should be kept low; in practical terms, this
 110 may mean that device size should be kept small. Competing with this are concerns over the survivability
 111 of the converter, which dictate that displacements of the WEC not be too large under severe conditions,
 112 favoring larger devices. We shall return to these issues in detail in later sections.

113 2.2. The Pierson Moskowitz spectrum

114 One of the most common descriptions of a sea-state for engineering purposes is the unidirectional
 115 Pierson Moskowitz (PM) spectrum, here given as a function of wavenumber k :

$$116 S(k) = \frac{0.00405}{k^3} \exp \left\{ -0.55411 \frac{g^2}{U^4 k^2} \right\}, \quad (3)$$

117 where U is the mean wind speed at a height of 10 m above the mean surface level, and g is the gravitational
 118 acceleration. This empirically derived formula gives the energy distribution for wind waves in deep water,
 119 and differs from the JONSWAP spectrum only by the addition of a spectral-peak enhancement factor.

120 This spectrum (3) readily yields a number of important values associated with the sea-state:

$$121 H^{(1/3)} = 0.24181U^2/g, \quad (4)$$

$$122 k_p = 0.66570g/U^2, \quad (5)$$

123 where $H^{(1/3)}$ is the significant wave height and k_p is the wave number of the spectral peak for a given
 124 wind speed U . This makes it easy to present subsequent results in an alternative form when desired. A
 125 monochromatic wave with wavenumber k_p and the same wave energy density as the PM spectrum will
 126 have an amplitude

$$127 a_0(k_p) = 0.08549U^2/g. \quad (6)$$

128 For subsequent illustration it will be necessary to have some concrete, physical examples, which means
 129 specifying a sea-state via a wind speed value U . Our design conditions (denoted by a subscript d) will
 130 correspond to a wind speed $U_d = 10$ m/s, while we will consider two “severe states” (denoted by subscripts
 131 $s1$ and $s2$) with regard to the survivability, corresponding to wind speeds $U_{s1} = 15$ m/s and $U_{s2} = 20$
 132 m/s. These are summarized in Table 1.

Table 1: The wind speed U , significant wave height $H^{(1/3)}$, peak wavenumber k_p , and peak wavelength $\lambda_p = 2\pi/k_p$ associated with PM spectra used for design and survivability considerations.

	S_d	S_{s1}	S_{s2}
U (m/s)	10	15	20
$H^{(1/3)}$ (m)	2.47	5.55	9.87
k_p (1/m)	0.065	0.029	0.016
λ_p (m)	96.30	216.67	385.19

3. Governing equations

Our approach to solving the wave-structure problem for the twin-cylinder WEC relies on domain decomposition and eigenfunction expansion methods (in the context of floating cylinders, see Black & Mei [20], who give a comprehensive description of the method, or more generally, Linton & McIver [21], or Zheng et al [16] for a recent application to floating cylinders). As the full formulation is rather lengthy, we only indicate the most important equations, and refer the interested reader to work cited above.

The fluid is assumed to be incompressible and inviscid, and the flow irrotational. Introducing a velocity potential $\Phi(r, \theta, z, t)$, and assuming periodic motion of frequency ω , the potential is separated into the spatial and temporal parts,

$$\Phi(r, \theta, z, t) = \phi(r, \theta, z)e^{i\omega t}, \quad (7)$$

where $\phi(r, \theta, z)$ satisfies the Laplace equation:

$$\phi_{rr} + \frac{1}{r}\phi_r + \frac{1}{r^2}\phi_{\theta\theta} + \phi_{zz} = 0, \quad (8)$$

subject to the linearized boundary conditions on the free surface $z = 0$ and on the bed $z = -h$:

$$\phi_z - \sigma\phi = 0, \quad \text{on } z = 0, \quad r > R, \quad (9)$$

$$\phi_z = 0, \quad \text{on } z = -h, \quad (10)$$

where $\sigma = \omega^2/g$.

At the interface between structure and fluid, the normal velocity of the structure must equal that of the adjacent fluid particles, written in terms of the potential (7):

$$\frac{\partial\Phi}{\partial n} = V_n, \quad (11)$$

where V_n is the component of the structure's velocity in the direction of the outward pointing normal vector n , which may be applied at the equilibrium surface under the assumptions of linearity. Owing to this very linearity, we continue with a decomposition of the problem into two parts: one due to the waves (ϕ_S) scattered from the structure (which is assumed fixed) by the incident wave field, and one due to the waves (ϕ_R) radiated by the motion of the structure, such that $\phi = \phi_S + \phi_R$. ϕ_S is decomposed further into the potential due to the incident wave ϕ_I and that due to the waves diffracted from the fixed structure ϕ_D , where

$$\frac{\partial \phi_D}{\partial n} = -\frac{\partial \phi_I}{\partial n} \text{ on the body surface } S. \quad (12)$$

The remaining radiated part of the potential ϕ_R must then satisfy (11), where the normal velocities are to be determined from the equations of motion. We shall consider an incident monochromatic wave with amplitude a_0 , so that ϕ_I is known *a priori*.

Introducing the as-yet unknown displacements of the upper ($j = 1$) and lower ($j = 2$) cylinder for the three modes of motion

$$\zeta_{zj} = \zeta_{zj0} e^{i\omega t} \text{ for heave,} \quad (13)$$

$$\zeta_{xj} = \zeta_{xj0} e^{i\omega t} \text{ for sway,} \quad (14)$$

$$\theta_j = \theta_{j0} e^{i\omega t} \text{ for roll,} \quad (15)$$

where ζ_{zj0} , ζ_{xj0} and θ_{j0} are the complex amplitudes of the corresponding displacements, we can write the boundary condition (11) for the spatial part of the total potential ϕ in the following form

$$\phi_z = i\omega\zeta_{z10} - i\omega\theta_{10}r \cos \theta, \quad \text{on } z = -H_1, r < R, \quad (16)$$

$$\phi_z = i\omega\zeta_{z20} - i\omega\theta_{20}r \cos \theta, \quad \text{on } z = -(H_1 + H_2), z = -(H_1 + H_2 + H_3), r < R \quad (17)$$

$$\phi_r = i\omega\zeta_{x10} \cos \theta - i\omega\theta_{10}(z_0 - z) \cos \theta, \quad \text{on } -H_1 < z < 0, r = R, \quad (18)$$

$$\phi_r = i\omega\zeta_{x20} \cos \theta - i\omega\theta_{20}(z_0 - z) \cos \theta, \quad \text{on } -(H_1 + H_2 + H_3) < z < -(H_1 + H_2), r = R, \quad (19)$$

where (16) is posed on the bottom of the upper cylinder, (17) on the top and bottom of the lower cylinder, (18) on the sides of the upper cylinder, and (19) on the sides of the lower cylinder. These conditions are supplemented by Sommerfeld's radiation condition, requiring the diffracted and radiated waves to be outgoing as $r \rightarrow \infty$. Due to the configuration of two axisymmetric floating cylinders, we must consider three fluid regions, one between the coaxial cylinders (region II), one between the lower cylinder and the

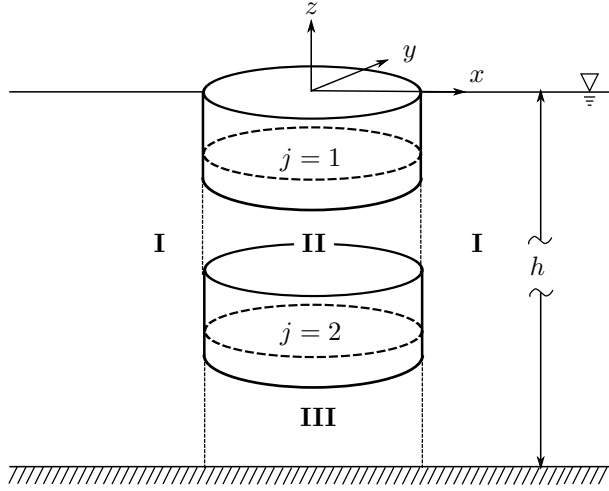


Figure 2: Domain decomposition for the twin-cylinder problem.

141 bed (region III), and one outside the vertical extension of the cylinders (region I), as depicted in Figure
 142 2. Subsequently the scattering problem is divided into three problems, one in each subdomain, and the
 143 radiation problem for each of the three modes of each of the two cylinders is divided into three problems.
 144 The reader may appreciate the effort involved in keeping track of, solving, and subsequently matching
 145 solutions, of 21 problems for the potentials involved. These potentials are then applied in calculating the
 146 forces on the two cylinders, in the form of pressures from the surrounding fluid.

147 The full expressions for the exciting, hydrodynamic, and hydrostatic forces are lengthy and will not
 148 be given. We note only that we have found excellent agreement between our results and published work
 149 [5, 7, 10, 16, 8, 11, 22].

The forces due to the fluid, together with those due to the dampers are employed with Newton's
 second law to yield the body motions. The first two equations, (20)-(21), equate the vertical (heave)
 forces with the masses and accelerations of the upper and lower cylinder, respectively. The next, (22)-
 (23), are those for the horizontal (sway) forces. The final pair, (24)-(25), equate the torques about the

y -axis to the angular acceleration times moment of inertia of the upper and lower cylinder, respectively.

$$F_{z1} + F_{z1 \rightarrow z1} + F_{z2 \rightarrow z1} + F_{hs,z1} + F_{d,z1} = -\omega^2 \zeta_{z10} M_1, \quad (20)$$

$$F_{z2} + F_{z1 \rightarrow z2} + F_{z2 \rightarrow z2} + F_{hs,z2} + F_{d,z2} = -\omega^2 \zeta_{z20} M_2, \quad (21)$$

$$F_{x1} + F_{x1 \rightarrow x1} + F_{x2 \rightarrow x1} + F_{y1 \rightarrow x1} + F_{y2 \rightarrow x1} = -\omega^2 \zeta_{x10} M_1, \quad (22)$$

$$F_{x2} + F_{x1 \rightarrow x2} + F_{x2 \rightarrow x2} + F_{y1 \rightarrow x2} + F_{y2 \rightarrow x2} = -\omega^2 \zeta_{x20} M_2, \quad (23)$$

$$F_{y1} + F_{x1 \rightarrow y1} + F_{x2 \rightarrow y1} + F_{y1 \rightarrow y1} + F_{y2 \rightarrow y1} + F_{hs,y1} + F_{d,y1} = -\omega^2 \theta_{10} I_1, \quad (24)$$

$$F_{y2} + F_{x1 \rightarrow y2} + F_{x2 \rightarrow y2} + F_{y1 \rightarrow y2} + F_{y2 \rightarrow y2} + F_{hs,y2} + F_{d,y2} = -\omega^2 \theta_{20} I_2, \quad (25)$$

The terms appearing in the above equations are given in Table 2.

$M_i, i \in \{1, 2\}$	Mass of cylinder i .
$I_i, i \in \{1, 2\}$	Moment of inertia of cylinder i about the y -axis.
$F_{xi}, F_{yi}, F_{zi}, i \in \{1, 2\}$	Exciting forces/torques on cylinder i in the x, y , and z directions
$F_{\alpha i \rightarrow \beta j}, i, j \in \{1, 2\}, \alpha, \beta \in \{x, y, z\}$	Hydrodynamic force/torque of the α motion of cylinder i in the β direction of cylinder j .
$F_{hs,yi}, F_{hs,zi}, i \in \{1, 2\}$	Hydrostatic forces/torques in the y and z direction on cylinder i .
$F_{d,yi}, F_{d,zi}, i \in \{1, 2\}$	Forces/torques caused by the damping system in the y and z direction on cylinder i .
$\zeta_{xi0}, \zeta_{zi0}, \theta_{i0}, i \in \{1, 2\}$	Displacement amplitudes of cylinder i in sway (ζ_x), heave (ζ_z), and roll (θ).

Table 2: Notation for terms appearing in (20)–(25). Terms with subscripted x or z are forces, and terms with subscripted y are torques.

The masses and moments of inertia have the explicit form (see (1), (2))

$$M_1 = M_2 = \rho \pi q^3,$$

$$I_1 = \frac{73}{108} \rho \pi q^5,$$

$$I_2 = \frac{757}{108} \rho \pi q^5,$$

and the damping forces are

$$F_{d,z1} = -i\omega C(\zeta_{z10} - \zeta_{z20})e^{i\omega t},$$

$$F_{d,z2} = i\omega C(\zeta_{z10} - \zeta_{z20})e^{i\omega t},$$

$$F_{d,y1} = -\frac{1}{2}i\omega CR^2(\theta_{10} - \theta_{20})e^{i\omega t},$$

$$F_{d,y2} = \frac{1}{2}i\omega CR^2(\theta_{10} - \theta_{20})e^{i\omega t}.$$

After the displacements of the cylinders are obtained, the captured power can then be calculated as follows:

$$P_a = \frac{1}{2}C\omega^2(\zeta_{z10} - \zeta_{z20})(\zeta_{z10}^* - \zeta_{z20}^*) + \frac{1}{4}C\omega^2 R^2(\theta_{10} - \theta_{20})(\theta_{10}^* - \theta_{20}^*), \quad (26)$$

where ζ_{zj0}^* and θ_{j0}^* are the complex conjugates of ζ_{zj0} and θ_{j0} , respectively.

4. Design of the WEC for monochromatic waves

We now undertake to examine the design of the WEC, based on the three parameters characterizing the environmental conditions ρ , g , and U , the two WEC parameters q and C , and the seven WEC performance parameters calculated from the wave-structure interaction problem P_a , ζ_{x10} , ζ_{x20} , ζ_{z10} , ζ_{z20} , θ_{10} and θ_{20} .

An application of Buckingham's π theorem [23] yields that there will be nine dimensionless quantities that characterize this problem: $\frac{q}{U^2/g}$, $\frac{C}{\rho U^5/g^2}$, $\frac{P_a}{\rho U^7/g^2}$, $\frac{\zeta_{zj0}}{U^2/g}$, $\frac{\zeta_{xj0}}{U^2/g}$, and θ_{j0} , where $j \in \{1, 2\}$ again denotes the upper and lower cylinder, respectively. In the sequel, we will make use of a \sim to denote nondimensional variables, i.e., the nine dimensionless quantities above will be \tilde{q} , \tilde{C} , \tilde{P}_a , $\tilde{\zeta}_{zj0}$, $\tilde{\zeta}_{xj0}$, and $\tilde{\theta}_{j0}$.

4.1. The WEC in heave motion under a monochromatic wave

For simplicity of presentation and ease of understanding we initially consider only the heave mode, motivated by the fact that, while sway and roll are generally coupled, they are both independent of heave. The response of the WEC under incoming monochromatic waves is first considered, where our physical test-case corresponds to a monochromatic wave of wavelength 96.3 m (equal to that at the peak of the design spectrum S_d) and an amplitude $a_d = 0.87$ m, such that the total energy density of the wave is equal to that of S_d , see (6) and Table 1.

167 4.1.1. Step 1: determination of the WEC's size

1 We first choose the dashpot coefficient C to be zero, which means that the two cylinders are freely
 2 floating. In this case, once the incident monochromatic wave is given, the only WEC parameter to be
 3 determined is q . Dimensional analysis can then be applied to the problem of determining the quantity
 4 of interest q for the motions of the upper cylinder ζ_{z10} and the lower cylinder ζ_{z20} separately. Once
 5 again, Buckingham's π theorem yields that, for the variables ρ, g, U, q , and ζ_{zj0} , there exist exactly two
 6 nondimensional quantities, which must be related by a relation
 7
 8
 9
 10
 11
 12
 13

$$\tilde{\zeta}_{zj0} = \Psi_{1j}(\tilde{q}). \quad (27)$$

168 The maximum displacement of the cylinder j as a function of size \tilde{q} thus corresponds to the extrema of
 169 Ψ_1 . Equation (27) is plotted in Figure 3 for the upper and lower cylinders.
 20
 21
 22
 23
 24

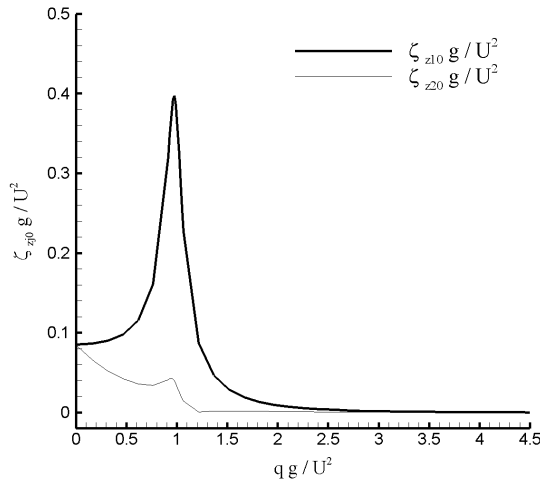


Figure 3: Displacement amplitudes for each of the two freely floating cylinders ($C = 0$) under the design monochromatic wave. $\tilde{\zeta}_{z10}$: upper cylinder, thick line; $\tilde{\zeta}_{z20}$: lower cylinder, thin line.

170 As we are ultimately interested in relative displacements of the cylinders, the global maximum of
 171 $\Psi_{11}(\tilde{\zeta}_{z10})$ and the local maximum of $\Psi_{12}(\tilde{\zeta}_{z20})$ which occur at $\tilde{q} = 0.97$ yield the chosen design size.
 172
 173

172 4.1.2. Step 2: determination of the dashpot coefficient C

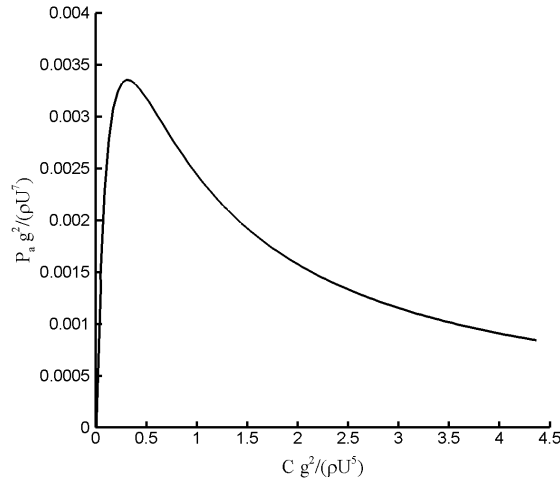
173 The maximum displacement in Fig. 3 is related to the resonance between the cylinders and the incident
 174 monochromatic wave. The introduction of a damper, while changing the magnitude of the displacement,
 175 can be shown to have no effect on the location of the resonant maximum, which remains $\tilde{q} = 0.97$ (see
 176 Fig. 3) even for various values of C . Thus, the size of the WEC determined from the freely floating case
 177
 178

177 is used to specify the damping coefficient C .

1
2 Given the unique relationship between q and ζ_{zj0} , independent of C , described above, the dimensional
3 analysis yields an equation

$$\tilde{P}_a = \Psi_2(\tilde{C}; \tilde{q}), \quad (28)$$

178 where Ψ_2 is plotted in Fig. 4 for the WEC size as determined in the last section ($\tilde{q} = 0.97$).



30 Figure 4: The relationship between the captured power \tilde{P}_a and the dashpot coefficient \tilde{C} for the heave motion induced by
31 the design monochromatic wave, where $\tilde{q} = 0.97$.

179 We elect to determine the dashpot coefficient C from the maximum of captured power P_a in Figure
36 4, calculated from the heave terms only in (26). This results in $\tilde{C} = 0.32$ and $\tilde{P}_a = 0.0034$.

180 Thus, the WEC design for a monochromatic wave has been determined. Taking the design wave
39 introduced in the beginning of Section 4 as a physical example, the WEC has the dimensions $q = 9.9m$
41 and $C = 3.3 \times 10^5 Ns/m$, and can capture $P_a = 3.5 \times 10^5$ Watt from a monochromatic wave 96.3 m long
43 and 0.87 m in amplitude.
46

185 4.2. General motions of the WEC in monochromatic waves

186 Having treated the simpler case of heave-only motion, we now consider the general case in which the
52 WEC is additionally allowed to undergo sway and roll motions. Akin to the previous section which only
53 dealt with the heave motion, the design procedure of the WEC in the general case is also divided into
55 two steps, as illustrated in detail below.
58

190 *4.2.1. Step 1: Determination of the WEC's size q*

191 We start once again with the freely floating case, where the dashpot coefficient $C = 0$. Using the
 192 equations of motion (20)-(25), we can obtain the displacements of the two cylinders in the x and z
 193 directions, and the angle around the y axis.

194 Once the monochromatic wave is given, or equivalently, once the mean wind speed for the corre-
 195 sponding PM spectrum is given (recall that this can be used to specify a monochromatic wave for design
 196 purposes by (6)), the physical process of determining the size of the WEC can be written in the following
 197 dimensionless form:

$$\tilde{\zeta}_{zj0} = \Psi_{1j}(\tilde{q}), \quad (29)$$

$$\tilde{\zeta}_{xj0} = \Psi_{2j}(\tilde{q}), \quad (30)$$

$$\theta_{j0} = \Psi_{3j}(\tilde{q}), \quad (31)$$

198 where ζ_{zj0} and ζ_{xj0} denote the amplitudes of the vertical and horizontal displacements respectively, θ_{j0}
 199 is the amplitude of the angle around the y axis, and $j = 1, 2$ corresponds to the upper and lower cylinder,
 200 respectively. We now seek the maxima of the functions Ψ_{1j}, Ψ_{2j} and Ψ_{3j} , which correspond to the six
 201 curves presented in Fig.5.

202 Due to the increase in number of modes, the picture of the displacements is more complex than in the
 203 preceding section. It may be observed that the heave mode is decoupled from the sway and roll modes,
 204 yielding again the global maximum at $\tilde{q} = 0.97$. The sway and roll modes are coupled, and are observed
 205 to present a global maximum for relative displacement at $\tilde{q} = 0.61$, resulting in an ambiguous situation
 206 for determining the size of the WEC.

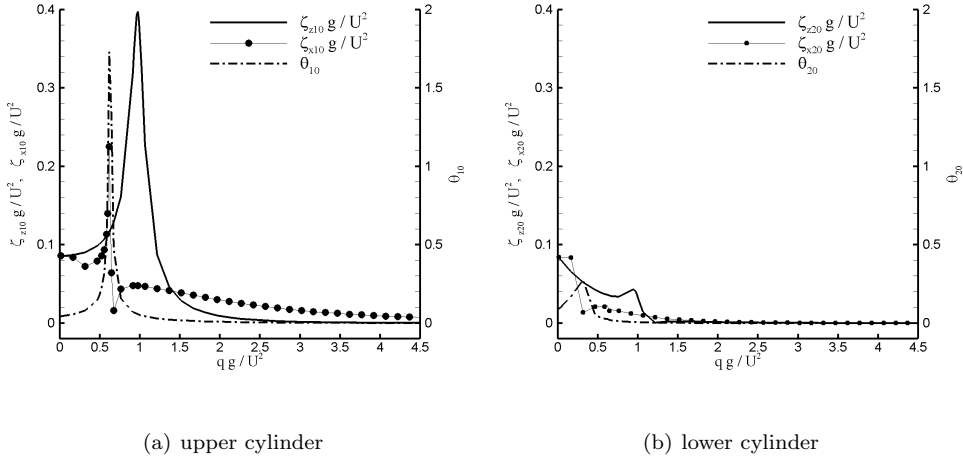


Figure 5: Displacement amplitudes of the two freely-floating cylinders ($C = 0$) in heave, sway and roll under the design monochromatic wave. $\tilde{\zeta}_{zj0}$: amplitude of the vertical displacement; $\tilde{\zeta}_{xj0}$: amplitude of the horizontal displacement; θ_{j0} : amplitude of the angle around the y axis. $j = 1, 2$ correspond to the upper and lower cylinders, respectively.

4.2.2. Step 2: Determination of the dashpot coefficient C

As in the preceding section, we now suppose that the size of the WEC is given. The captured power P_a then depends on the dashpot coefficient C . The determination of optimal power absorption as a function of dashpot coefficient is described in dimensionless form by

$$\tilde{P}_a = \Psi_4(\tilde{C}; \tilde{q}), \quad (32)$$

where, as we have seen, there is some flexibility in choice of q . The function Ψ_4 is plotted in Fig. 6 for both $\tilde{q} = 0.61$ and $\tilde{q} = 0.97$. For the device operating optimally in heave ($\tilde{q} = 0.97$, thick line) there is a unique maximum at $\tilde{C} = 0.34$ with $\tilde{P}_a = 0.0035$ (denoted Case E), very close to the heave-only case discussed in Section 4.1. For the roll-sway optimized device ($\tilde{q} = 0.61$, thin line) there are two local maxima $\tilde{C} = 0.035$ and $\tilde{C} = 1.34$, with corresponding $\tilde{P}_a = 0.0012$ and 0.0013 , (denoted Case A1 and A2, respectively).

The situation for monochromatic incident waves is summed up in Table 3, which shows the nondimensional size, optimal damping, captured power, and displacement amplitudes for the cases discussed above. As we have observed, introducing roll and sway motions leads to a two-fold branching in the design procedure. Firstly, in free motion, one value of \tilde{q} is found to yield the largest roll and sway displacements, while another value yields the largest heave displacements. While the heave-optimized case has a unique maximum \tilde{P}_a as a function of damping, the roll/sway-optimized case admits two local maxima of \tilde{P}_a , one

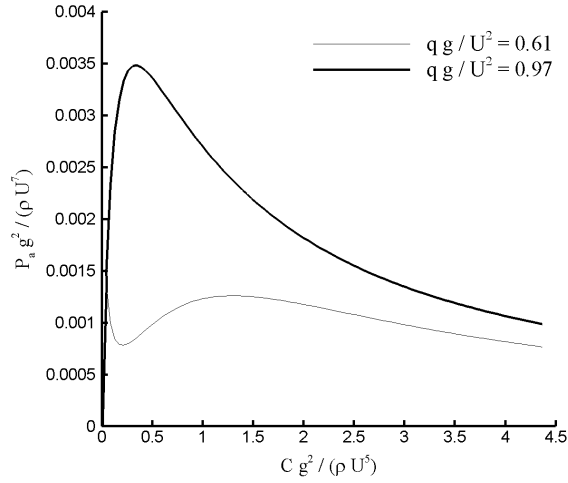


Figure 6: The captured power P_a of the WEC in the combined motions versus the dashpot coefficient C . Thin line: $\frac{q}{U^2/g} = 0.61$; thick line: $\frac{q}{U^2/g} = 0.97$.

with relatively low, the other with relatively high damping \tilde{C} , compared to the heave case (see Figure 6).

This opens up the possibility that the overall optimal design may not coincide with a design optimized for roll/sway or heave alone, but occupying some middle ground. The performance of such intermediate devices (Cases B, C, and D), as well as devices somewhat larger than Case E (Cases F, G and H) is explored for the monochromatic design wave in Table 3. In each of Cases B through H, a damping C has been chosen to maximize the captured power.

Table 3: The size, damping, captured power and displacement of 3-mode WECs in monochromatic waves.

Cases:	A1	A2	B	C	D	E	F	G	H
\tilde{q}	0.61	0.61	0.70	0.79	0.88	0.97	1.06	1.15	1.24
\tilde{C}	0.035	1.34	0.90	0.67	0.51	0.34	0.56	1.09	1.91
\tilde{P}_a	0.0012	0.0013	0.0015	0.0021	0.0028	0.0035	0.0028	0.0020	0.0015
$\tilde{\zeta}_{z10}$	0.11	0.089	0.093	0.11	0.14	0.19	0.13	0.063	0.039
$\tilde{\zeta}_{z20}$	0.036	0.053	0.033	0.026	0.023	0.021	0.0097	0.0042	0.0031
$\tilde{\zeta}_{x10}$	0.12	0.063	0.060	0.055	0.050	0.048	0.047	0.040	0.038
$\tilde{\zeta}_{x20}$	0.018	0.016	0.015	0.013	0.012	0.011	0.0093	0.0069	0.0057
$\theta_{10}(rad)$	0.70	0.041	0.052	0.069	0.068	0.056	0.042	0.028	0.022
$\theta_{20}(rad)$	0.028	0.031	0.021	0.014	0.0094	0.0066	0.0051	0.0035	0.0027

Here we see that a shift in device size from the smaller, primarily rolling/swaying devices, towards larger, primarily heaving devices has a positive impact on captured power, up to device E. Thereafter, an increase in device size leads to a reduction in captured power, as the larger devices operate preferentially at smaller wavenumbers.

230 This situation is depicted in Figure 7, which shows $\tilde{P}_a^* \equiv P_a^*/(\rho U^3)$, the dimensionless captured power
 1 per unit wave amplitude squared, where $P_a^* \equiv P_a/a_0^2$. To illustrate the associated displacements, Figure
 2 231 per unit wave amplitude squared, where $P_a^* \equiv P_a/a_0^2$. To illustrate the associated displacements, Figure
 3 8 shows the displacement in heave for the upper cylinder ζ_{z10} divided by a_0 . Note that for case A1, the
 4 232 maximum value of $\zeta_{z10}(k)/a(k)$ is 4.4 (not shown).
 5
 6 233 maximum value of $\zeta_{z10}(k)/a(k)$ is 4.4 (not shown).
 7
 8
 9

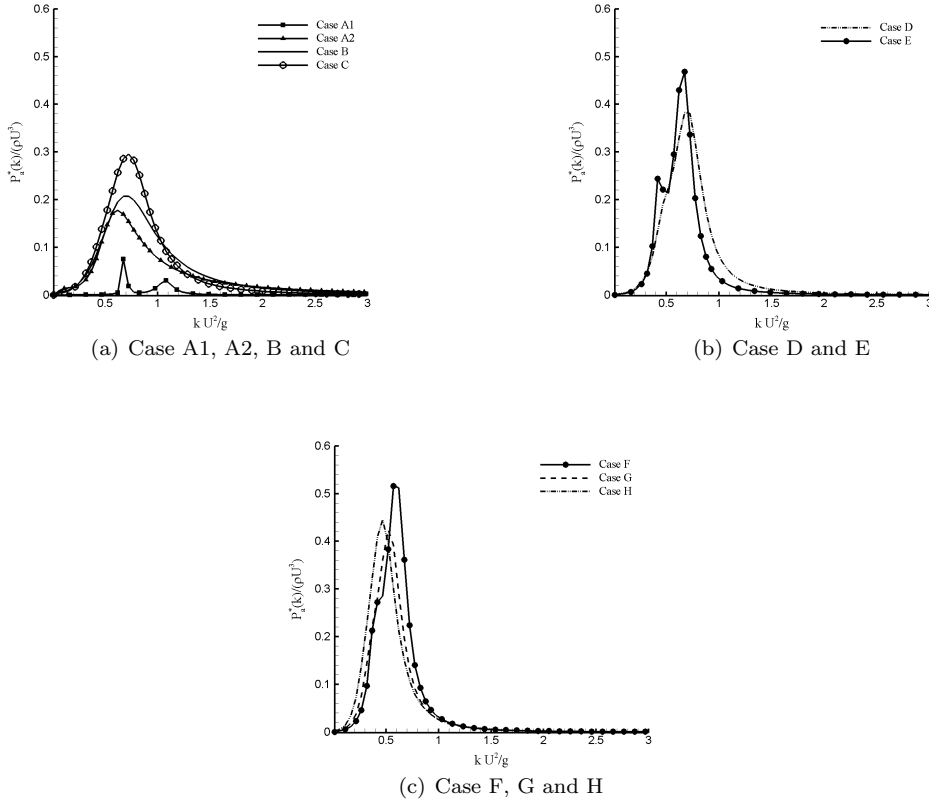


Figure 7: The dimensionless captured power per unit wave amplitude square $P_a^*(k)/(\rho U^3)$ under different monochromatic waves as a function of wavenumber.

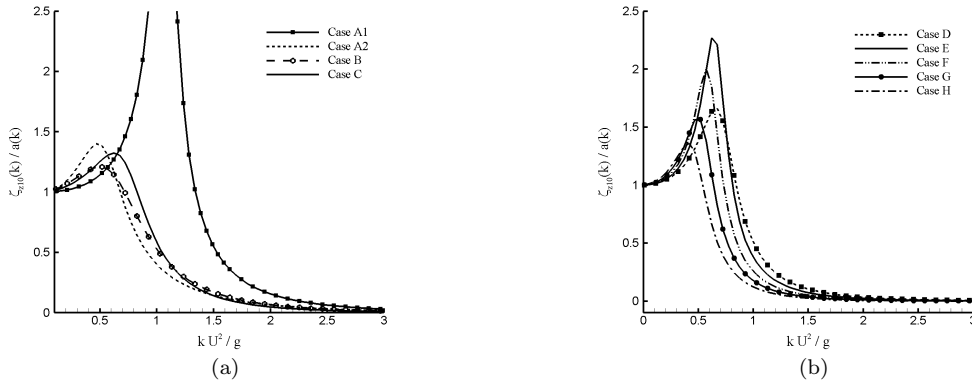


Figure 8: The dimensionless displacement $\hat{A}_{z1} = \zeta_{z10}/a_0$ of the upper cylinder in the combined motions under different monochromatic waves. (a) vertical displacement of cases A1, A2, B and C; (b) vertical displacement of cases D, E, F, G and H.

5. Design of the WEC for a PM spectrum

Up to this point, we have considered WEC design for monochromatic waves. In brief: a given wind speed U determines the two necessary parameters, wavenumber k_p and amplitude a_0 from (6). With a monochromatic wave fully described by (k_p, a_0) , we may initially assume freely floating cylinders, and choose their size \tilde{q} for maximum displacement in roll and sway (as these modes are coupled), for maximum displacement in heave, or at some intermediate value. In each case, a damping \tilde{C} is chosen to maximize the captured power for this incident design wave, leading to the cases A1 through H above. As demonstrated in Figures 7 and 8, the motions and performance of a device designed for a wave $(k_p, a_0(k_p))$ may change considerably for other waves.

For practical reasons, our primary interest must be focused on irregular waves, where we may elect to tune the device to operate optimally at the peak of the spectrum, but must consider its performance for a broad band of incident waves. Under irregular waves it is no longer possible to give a single value for the displacements of each floating cylinder. We begin with some preliminaries regarding the behavior of the WEC in irregular seas.

For a monochromatic wave, the absorbed power P_a (see (26)) and displacements $\zeta_{\alpha j 0}$ are written as

$$P_a(q, C, k, a_0) \equiv a_0^2 P_a^*(q, C, k),$$

$$\zeta_{\alpha j 0}(q, C, k, a_0) \equiv a_0 \hat{A}_{\alpha j}(q, C, k),$$

$$\theta_{j 0}(q, C, k, a_0) \equiv a_0 \hat{A}_{y j}(q, C, k).$$

where $j = 1, 2$ denotes the upper and lower cylinders, P_a^* is the absorbed power per unit wave amplitude square, and $\hat{A}_{\alpha j}$ with $\alpha \in \{x, y, z\}$ denote the relative amplitudes of sway, roll and heave motions, respectively. For a given spectrum $S(k)$ the total absorbed power by a device of type (q, C) is

$$P_a^{\text{total}} = \int_0^\infty 2P_a^*(k)S(k)dk. \quad (33)$$

Just as the spectrum describes the distribution of wave energy among different frequencies, and allows for statistical inferences such as a definition of the significant wave-height, so analogously we may consider a *displacement spectrum*

$$E_{\alpha j}(k) \equiv S(k)(\hat{A}_{\alpha j})^2, \quad (34)$$

and define the *significant displacement* by

$$H_{\alpha j}^{1/3} = 4 \cdot \left(\int_0^\infty E_{\alpha j}(k)dk \right)^{1/2}. \quad (35)$$

Here $H_\alpha^{(1/3)}$ ($\alpha = x, y, z$) is the the distance from the displacement's trough to crest and

$$\zeta_{z j 0}^{(1/3)} = \frac{1}{2} H_{z j}^{(1/3)}, \quad (36)$$

$$\zeta_{x j 0}^{(1/3)} = \frac{1}{2} H_{x j}^{(1/3)}, \quad (37)$$

$$\theta_{j 0}^{(1/3)} = \frac{1}{2} H_{y j}^{(1/3)}, \quad (38)$$

are the so-called “significant amplitudes of the displacement” in z and x directions, and the angle around y axis, respectively.

Applying the concepts developed above to the problem of power absorption from an incident, broad-banded sea, we evaluate the above expressions for the spectra introduced in Section 2. The results are given in nondimensional form in Table 4, which shows the captured power and displacement amplitudes for the spectra S_d , S_{s1} and S_{s2} , nondimensionalized by $U = U_d$. This may be compared to the analogous Table 3 for the monochromatic case. In the following section, we turn to a discussion of these results.

Table 4: The dimensionless captured power $\tilde{P}_a^{\text{total}}$ along with nondimensional significant amplitudes of displacement in heave $\zeta_{zj0}^{(1/3)}$, sway $\zeta_{xj0}^{(1/3)}$, and roll $\theta_{j0}^{(1/3)}$ (rad), for the WECs A1 through H attacked by a design spectrum S_d , a severe spectrum S_{s1} ($U_{s1} = 1.5U_d$), and a second severe spectrum S_{s2} ($U_{s2} = 2U_d$).

Cases:	A1	A2	B	C	D	E	F	G	H
\tilde{q}	0.61	0.61	0.70	0.79	0.88	0.97	1.06	1.15	1.24
\tilde{C}	0.035	1.34	0.90	0.67	0.51	0.34	0.56	1.09	1.91
<i>S_d</i>									
$\tilde{P}_a^{\text{total}}$	7.01×10^{-5}	0.00065	0.00081	0.0010	0.0011	0.0010	0.0011	0.00089	0.00086
$\zeta_{z10}^{(1/3)}$	0.22	0.097	0.096	0.11	0.12	0.14	0.12	0.094	0.071
$\zeta_{z20}^{(1/3)}$	0.044	0.065	0.040	0.030	0.027	0.025	0.021	0.017	0.013
$\zeta_{x10}^{(1/3)}$	0.10	0.077	0.073	0.068	0.064	0.059	0.056	0.054	0.051
$\zeta_{x20}^{(1/3)}$	0.022	0.019	0.018	0.016	0.015	0.014	0.012	0.011	0.0093
$\theta_{10}^{(1/3)}$	0.60	0.050	0.059	0.073	0.084	0.096	0.068	0.045	0.032
$\theta_{20}^{(1/3)}$	0.012	0.015	0.0093	0.0058	0.0039	0.0027	0.0020	0.0016	0.0012
<i>S_{s1}</i>									
$\tilde{P}_a^{\text{total}}$	0.00016	0.0025	0.0030	0.0037	0.0043	0.0046	0.0061	0.0060	0.0074
$\zeta_{z10}^{(1/3)}$	0.37	0.31	0.29	0.29	0.32	0.35	0.34	0.31	0.29
$\zeta_{z20}^{(1/3)}$	0.15	0.25	0.18	0.14	0.13	0.12	0.11	0.11	0.10
$\zeta_{x10}^{(1/3)}$	0.25	0.21	0.22	0.21	0.21	0.21	0.20	0.19	0.19
$\zeta_{x20}^{(1/3)}$	0.090	0.076	0.081	0.081	0.078	0.075	0.070	0.065	0.060
$\theta_{10}^{(1/3)}$	0.98	0.16	0.14	0.17	0.21	0.29	0.23	0.16	0.12
$\theta_{20}^{(1/3)}$	0.13	0.17	0.11	0.075	0.058	0.046	0.039	0.034	0.029
<i>S_{s2}</i>									
$\tilde{P}_a^{\text{total}}$	0.00019	0.0044	0.0049	0.0056	0.0064	0.0068	0.0097	0.011	0.014
$\zeta_{z10}^{(1/3)}$	0.55	0.54	0.51	0.52	0.53	0.56	0.56	0.54	0.53
$\zeta_{z20}^{(1/3)}$	0.34	0.47	0.39	0.33	0.30	0.29	0.28	0.27	0.27
$\zeta_{x10}^{(1/3)}$	0.45	0.42	0.42	0.42	0.42	0.42	0.42	0.41	0.40
$\zeta_{x20}^{(1/3)}$	0.20	0.19	0.19	0.20	0.20	0.19	0.19	0.18	0.17
$\theta_{10}^{(1/3)}$	1.07	0.317	0.21	0.22	0.27	0.37	0.31	0.24	0.19
$\theta_{20}^{(1/3)}$	0.31	0.40	0.25	0.18	0.14	0.12	0.10	0.088	0.077

6. Discussion

As have mentioned above, several competing criteria exist in determining WEC size. Those we shall consider in depth are limited to power capture, which naturally should be maximized, and survivability as assessed from the device motions.

We note that the Cases A1 through H presented above are ordered by increasing size q which may be assumed correlated to the cost *per device*, all other things being equal. Due to the burgeoning state of wave energy technology, it seems premature to speculate any further about cost, given that it depends not only on device size, but also design specifics such as materials and component costs, as well as costs

264 related to regular maintenance or major overhaul, both factors which will in turn be affected by size.

265 In the following sections, we will delve into a detailed analysis of the WEC behaviour with a view to
 266 power capture and survivability. Subsequently, a synthesis of these two viewpoints is attempted, bearing
 267 in mind the primary aim of providing quantitative information relating to the design of oscillating body
 268 converters in a range of different, broad-banded sea states.

269 6.1. Power capture

270 The most straightforward metric to evaluate concerns the power captured by a WEC. For a design PM
 271 spectrum S_d corresponding to a wind speed $U_d = 10$ m/s, and severe spectra S_{s1} and S_{s2} corresponding
 272 to $U_{s1} = 15$ m/s and $U_{s2} = 20$ m/s, respectively, the dimensional size, damping and absorbed power of
 273 WECs A1 through H are presented in Table 5.

Table 5: Dimensional absorbed power P_a (Watt) for cases A1 through H, for an incoming monochromatic wave (P_a^m) and the design PM spectrum with $U = 10$ m/s (P_a^d), both with the same energy density of 3.7 KJ/m². Also given are the absorbed power for the severe spectra S_{s1} (P_a^{s1}) and S_{s2} (P_a^{s2}).

Cases:	A1	A2	B	C	D	E	F	G	H
q [m]	6.2	6.2	7.1	8.1	9.0	9.9	10.8	11.4	12.7
C ($\cdot 10^5$) [Ns/m]	0.364	14.0	9.37	6.98	5.31	3.54	5.83	11.3	19.9
P_a^m ($\cdot 10^5$) [W]	1.25	1.35	1.56	2.19	2.92	3.64	2.92	2.08	1.56
P_a^d ($\cdot 10^5$) [W]	0.0730	0.672	0.849	1.04	1.14	1.06	1.17	0.931	0.893
P_a^{s1} ($\cdot 10^5$) [W]	0.165	2.65	3.13	3.80	4.43	4.77	6.36	6.27	7.73
P_a^{s2} ($\cdot 10^5$) [W]	0.197	4.62	5.09	5.88	6.67	7.10	10.1	11.0	15.0

274 We recall the monochromatic wave used for device design, with a wavelength of 96.3 m and an
 275 amplitude of 0.87 m, with an energy density of 3.7 KJ/m² equal to that of the design PM spectrum
 276 parametrised by a wind-speed $U = 10$ m/s. The picture which emerges from comparing the absorbed
 277 powers in the monochromatic and spectral cases is quite striking. While the narrow-banded response of
 278 device A1 (see Figure 8(a)) yields a performance comparable to slightly larger devices for monochromatic
 279 waves, power absorption is dramatically lower for an incident PM spectrum.

280 Likewise, though the heave-optimized device E is clearly superior to devices of similar size (D and F)
 281 for monochromatic waves, this situation sees a dramatic reversal in the case of incident irregular waves.
 282 That devices either larger or smaller than the heave-optimum outperform it for irregular seas clearly
 283 demonstrates the pitfalls of a design based on monochromatic waves.

284 Dimensional values of captured power are also provided for the two severe spectra, S_{s1} corresponding

to a wind speed $U_{s1} = 15$ m/s, or an energy density of 18.7 KJ/m², as well as S_{s2} , corresponding to a wind speed $U_{s2} = 20$ m/s and an energy density of 59.6 KJ/m². As expected, the larger devices benefit most from this increased wave resource, while a sea composed of increasingly long waves (λ_p for S_{s1} is 217 m, and for S_{s2} is 385 m, see Table 1) begins to saturate the power capture capabilities of the smallest devices. In the following sections on survivability and grading of WECs, we shall explore the feasibility of operating WECs in such large sea states.

6.2. Survivability

We come now to the less well-defined of the two concepts with a bearing on the performance of a twin-cylinder WEC: survivability. The disparity between the motions and resulting loads experienced by a WEC in normal operation, and those during severe conditions may be immense. Following Brown et al [24] we distinguish between the reliability of a WEC, related to failure during normal operation, and survivability.

While it is clear that WECs must be robust in design, as during a ten-year operational period a converter may expect to see some tens of millions of waves, during particularly severe events, power production will need to be halted in order to avoid damage to the device or loss of station-keeping.

Table 6: Relative heave displacements versus draft $\zeta_z^r = (\zeta_{z10}^{(1/3)} - \zeta_{z20}^{(1/3)})/q$, and relative roll displacement $\theta^r = \theta_{10}^{(1/3)}/(\pi/2)$

	A1	A2	B	C	D	E	F	G	H
S_d									
ζ_z^r	0.29	0.05	0.08	0.10	0.11	0.12	0.09	0.07	0.05
θ_1	0.38	0.03	0.04	0.05	0.05	0.06	0.04	0.03	0.02
S_{s1}									
ζ_z^r	0.36	0.10	0.16	0.19	0.22	0.24	0.22	0.18	0.15
θ_1	0.62	0.10	0.09	0.11	0.13	0.18	0.15	0.10	0.08
S_{s2}									
ζ_z^r	0.34	0.11	0.17	0.24	0.26	0.28	0.26	0.24	0.21
θ_1	0.68	0.20	0.13	0.14	0.17	0.24	0.20	0.15	0.12

We have developed an example framework for survivability for the twin-cylinder WEC in the three spectral sea states considered, which is presented in Table 6. The maximum allowed relative vertical travel $\zeta_{z10}^{(1/3)} - \zeta_{z20}^{(1/3)}$ is limited to $q/3$, while the maximum allowable roll is 30°. Those cases which exceed these values are marked red (PDF only). A vertical travel between $q/4$ and $q/3$ or a roll between 22.5° and 30° is marked orange, while a vertical travel of between $0.15q$ and $0.25q$ or a roll between 13.5° and

22.5° is marked yellow (PDF only). Device motions smaller than these are marked green (PDF only).

Recall that these nondimensional quantities depend only on the relations $U_{s1} = 1.5 \cdot U_d$ and $U_{s2} = 2 \cdot U_d$ as specified in Section 2, and the concomitant changes in significant wave-height and peak wavenumber.

For illustrative purposes, if the design spectrum S_d is generated by a fresh breeze ($U_d = 10\text{m/s}$, or 5 Beaufort, 2.47 m $H^{(1/3)}$), then the first severe state S_{s1} may be thought generated by a high wind (7 Beaufort, 5.5 m $H^{(1/3)}$). The second severe state S_{s2} occurs under conditions between gale and severe gale (8–9 Beaufort, 9.9m $H^{(1/3)}$). These extremely harsh conditions represent an energy density more than 16 times that of the design spectrum, and may be expected to challenge the device design. Note that the nondimensional form of the results allows for a free choice of U_d depending on the conditions of interest.

While the increase in significant wave-height between the design spectrum S_d and the severe case S_{s2} may seem dramatic, there is no doubt that such conditions will be encountered within the operational life of a WEC. For example, while deep water conditions for the Eastern Mediterranean off Israel’s coasts may see significant wave heights greater than 2 m only 6 % of the time, and wave heights in summer rarely exceed 1–1.5 m, nevertheless storms with $H^{(1/3)}$ in excess of 5 m occur almost yearly. The 10-year return period significant wave height is nearly 7 m, which clearly falls within the expected operational life of a converter.

From a pure survivability standpoint, it is immediate only that the smallest converter A1 is not viable. In particular, the very small damping of this configuration (see Table 5), while allowing for efficient power capture from the roll mode, also leads to overly large displacements even for design conditions. With survivability as the central aim of design, larger structures will necessarily fare better, though the differences between devices D, E, and F are in practice rather small. While other authors (e.g. Maisondieu [25] or Brown et al [24]) have investigated survivability of WECs, they have been forced to do so without reference to the hydrodynamics and actual displacements of a floating device, but rather purely based on estimations of the incident wave power.

6.3. Grading WEC sizes

We shall now make a preliminary attempt to sum up the results of the preceding sections. The intricacies of WEC economics, as well as the many factors which are outside the scope of the present study, such as moorings, specifics of the PTO, control strategies, power conversion and transmission,

1
2
3
4
5
6
7
8
9
10
11
12
13
14
15
16
17
18
19
20
21
22
23
24
25
26
27
28
29
30
31
32
33
34 and other environmental factors from seasonal variability to extreme events, will need to be taken into
35 account for a fuller analysis. For specific full-fledged designs, detailed information about performance
36 and survival may be sought through tank testing of scaled devices and CFD simulations (see e.g.²⁶). In
37 addition, WEC cost will not be considered, and is likely to impact significantly the ultimate design.

38 The lessons to be drawn from our comparison will likely change as wave-power technology matures.
39 In a parallel with the development of wind power over the past four decades, current commercial and
40 prototype oscillating-body WECs may be rather small, and situated in shallow water with the intention
41 of keeping costs down. It may be expected that future developments will lead naturally to a move into
42 the more powerful wave-regimes further offshore (see Stiassnie et al [27] for a discussion).

43 As an example, while there is a 15 % reduction in absorbed power between Case E and Case H
44 (coincident with a 24 % increase in radius q) under the design spectrum, the corresponding increase in
45 absorbed power for severe case S_{s2} is upwards of 60 %. The fact that, off the Eastern Mediterranean
46 Coast, some 45 % of average wave power comes during storm events that occur only 5 % of the time
47 indicates the utility of the larger design [28]. This is compounded by the increase in potential survivability
48 of the larger devices as indicated in the previous section. On the other hand, focusing on less frequent,
49 high-energy sea-states may mean that the WEC is operating below capacity for significant portions of
50 time.

51 Depending on the variability of the wave-energy resource, more or less weight may ultimately be
52 given to each of the considerations just outlined. The fact that the larger devices exhibit smaller relative
53 motions may also be a benefit for their reliability, in terms of limiting loading during normal operation.
54 Ultimately, an effort will have to be made to weigh the additional cost of a larger device against the
55 increase in survivability. Both of these in turn will need to be weighed against the potential of continuing
56 operation during high-energy events, while sustaining a slight performance decrease for low-energy sea
57 states.

58 7. Conclusions

59 We have investigated in detail the hydrodynamics of a model WEC consisting of two floating, axisym-
60 metric cylinders connected at their upper and lower perimeters by a continuously distributed damper –
61 allowing power capture from heave and roll modes. While other authors have studied various aspects

1
2
3
4
5
6
7
8
9
362 of the problem of floating cylinders, the present work addresses for the first time a twin cylinder WEC
363 allowed to move in three degrees of freedom. The inclusion of a floating, submerged cylinder as a mechan-
364 ical reference for power extraction makes this design viable in deep water. With further development of
365 the wave energy industry, it may be anticipated that WECs will follow wind turbines in moving further
366 offshore, making such self-reacting devices more and more relevant [27].

10
11
12
13
14
15
16
17
18
19
20
21
22
367 Our design procedure initially focused on optimizing device behavior for a damper of constant charac-
368 teristic in monochromatic waves. At the outset, the heave-only case was considered, presenting a simple
369 situation where a single device (characterized by a size parameter q and a damping parameter C), coin-
370 ciding with the resonant maximum of a freely floating body, outperformed all others. Allowing the device
371 also to sway and roll was seen to introduce additional complexity, and a differentiation was observed
372 between devices operating preferentially in roll/sway and those operating preferentially in heave.

23
24
25
26
27
28
29
30
31
32
373 Despite the multiplicity of possible designs when the device is allowed to undergo heave, sway, and roll
374 motions, the monochromatic case presents a clear picture from the standpoint of power absorption: the
375 device closest to heave resonance is found to perform best. This conclusion is an artifact of the idealization
376 represented by the monochromatic theory – a fact established by the subsequent investigation of WEC
377 performance under an irregular sea.

33
34
35
36
37
38
39
40
41
42
43
44
45
378 For our design purposes, a Pierson-Moskowitz spectrum, characterized by wind speed, was chosen
379 to evaluate the designs obtained from the monochromatic case. Under this spectrum, the maxima of
380 absorbed power were found to shift markedly with respect to the monochromatic case, reflecting the need
381 for separate design considerations for real sea states. Larger values of absorbed power under the design
382 spectrum were found for devices slightly larger and slightly smaller than the monochromatic optimum,
383 raising the question of how to determine device sizing in light of other criteria.

46
47
48
49
50
51
52
53
54
55
56
57
58
59
60
61
62
63
64
65
384 To this end, we have devised some example metrics for grading the sizes of our twin-cylinder WEC. We
385 note that wave energy presents particular difficulties in many respects. While a fixed offshore structure
386 may be designed for survival with very high safety factors, this is inappropriate for oscillating body
387 WECs; by their nature, they must undergo the largest possible motions in order to extract energy. At
388 the same time, device loading should be minimized to avoid fatigue and failure. Taking into account
389 the fact that WECs may be expected to be operational for on the order of 25 years (see Starling [29]),
390 and it becomes clear that survival is a paramount issue. We have presented an example approach to

1
2
3
4
5
6
7
8
9
10
11
12
13
14
15
16
17
18
19
20
21
22
23
24
25
26
27
28
29
30
31
32
33
34
35
36
37
38
39
40
41
42
43
44
45
46
47
48
49
50
51
52
53
54
55
56
57
58
59
60
61
62
63
64
65

391 quantitatively evaluate the competing aims of survivability and power extraction within the framework
392 of our floating twin-cylinder device.

393 To a certain extent all renewable energy technologies, WECs more than most, cannot control their
394 operating conditions, but must work within their environment, subject to the resulting fluctuations of
395 the resource. It must be expected that, like wind turbines, oscillating body WECs will be designed with
396 a “survival mode”, when normal operation cease, and the device changes its characteristics in order to
397 avoid extreme loads. (We might note that overtopping WECs or oscillating water-columns, due to a
398 different working principle and resulting size, will likely have a very different survivability analysis than
399 oscillating body designs.) This may mean increasing the damping, altering the water plane area or mass
400 (see Stallard et al [30]), or other approaches (see Coe and Neary [31]). Due to the nascent state of
401 commercial wave-energy technology, it is difficult to offer concrete design recommendations based on the
402 results for floating twin-cylinders. Our discussion does bear out the fact that a slight over-engineering
403 may be preferable, given the large relative contribution of infrequent, high-energy events to the annual
404 energy budget at many sites, and the demands of survival and robustness. We believe these results to
405 be applicable more broadly to oscillating-body converters, constrained in size as they are by the incident
406 wavelength, indicated by the striking similarities in performance between our twin-cylinder configuration
407 and a single bottom-referenced cylinder.

408 **Acknowledgements**

409 This research was supported by the Israel Science Foundation (Grant 464/13).

- 410 [1] F. Cerveira, N. Fonseca, R. Pascoal, Mooring system influence on the efficiency of wave energy
411 converters, *International Journal of Marine Energy* 3-4 (2013) 65–81. doi:10.1016/j.ijome.2013.
412 11.006.
- 413 [2] F. Ursell, On the heaving motion of a circular cylinder on the surface of a fluid, *Quart. Journ. Mech.*
414 and *Applied Math.* 2 (1949) 218–231.
- 415 [3] R. G. Dean, F. Ursell, Interaction of a fixed semi-immersed circular cylinder with a train of surface
416 waves, Tech. rep., MIT Hydrodynamics Laboratory Tech. Rep. no. 37 (1959).
- 417 [4] J. Miles, F. Gilbert, Scattering of gravity waves by a circular dock, *Journal of Fluid Mechanics* 34
418 (1968) 783–793.

- 1
2
3
4
5
6
7
8
9
10
11
12
13
14
15
16
17
18
19
20
21
22
23
24
25
26
27
28
29
30
31
32
33
34
35
36
37
38
39
40
41
42
43
44
45
46
47
48
49
50
51
52
53
54
55
56
57
58
59
60
61
62
63
64
65
- 419 [5] C. J. R. Garrett, Wave forces on a circular dock, *Journal of Fluid Mechanics* 46 (1971) 129–139.
- 420 [6] J. L. Black, C. C. Mei, M. C. G. Bray, Radiation and scattering of water waves by rigid bodies,
421 *Journal of Fluid Mechanics* 46 (1) (1971) 151–164. doi:10.1017/S0022112071000454.
- 422 [7] R. W. Yeung, Added mass and damping of a vertical cylinder in finite-depth waters, *Applied Ocean*
423 *Research* 3 (3) (1981) 119–133.
- 424 [8] D. D. Bhatta, Computation of added mass and damping coefficients due to a heaving cylinder,
425 *Journal of Applied Mathematics and Computing* 23 (1-2) (2007) 127–140.
- 426 [9] W. Finnegan, M. Meere, J. Goggins, The wave excitation forces on a truncated vertical cylinder
427 in water of infinite depth, *Journal of Fluids and Structures* 40 (2013) 201–213. doi:10.1016/j.
428 *jfluidstructs*.2013.04.007.
- 429 [10] L. Berggren, M. Johansson, Hydrodynamic coefficients of a wave energy device consisting of a buoy
430 and a submerged plate, *Applied Ocean Research* 14 (1) (1992) 51–58.
- 431 [11] X. Garnaud, C. Mei, Comparison of wave power extraction by a compact array of small buoys and
432 by a large buoy, *IET Renewable Power Generation* 4 (6) (2010) 519–530. doi:10.1049/*iet-rpg*.
433 2009.0166.
- 434 [12] B. F. M. Child, V. Venugopal, Optimal configurations of wave energy device arrays, *Ocean Engi-*
435 *neering* 37 (16) (2010) 1402–1417. doi:10.1016/j.*oceaneng*.2010.06.010.
- 436 [13] B. Borgarino, A. Babarit, P. Ferrant, Impact of wave interactions effects on energy absorption in large
437 arrays of wave energy converters, *Ocean Engineering* 41 (2012) 79–88. doi:10.1016/j.*oceaneng*.
438 2011.12.025.
- 439 [14] B. Teillant, R. Costello, J. Weber, J. Ringwood, Productivity and economic assessment of wave
440 energy projects through operational simulations, *Renewable Energy* 48 (2012) 220–230. doi:10.
441 1016/j.*renene*.2012.05.001.
- 442 [15] J. Engström, M. Eriksson, J. Isberg, M. Leijon, Wave energy converter with enhanced amplitude
443 response at frequencies coinciding with Swedish west coast sea states by use of a supplementary
444 submerged body, *Journal of Applied Physics* 106 (6). doi:10.1063/1.3233656.